Supplementary Data for:

The effect of macromolecular crowding on single-round transcription by *E. coli* RNA polymerase

SangYoon Chung[1], Eitan Lerner[1,9], Yan Jin[1], Soohong Kim[7,8], Yazan Alhadid[5], Logan Wilson Grimaud[1], Irina X. Zhang[1], Charles M. Knobler[1], William M. Gelbart[1,2,3,5]*, Shimon Weiss[1,2,3,4,5,6]*

[1]Department of Chemistry and Biochemistry, University of California Los Angeles, CA 90095, USA

[2]Molecular Biology Institute (MBI), University of California Los Angeles, CA 90095, USA

[3]California NanoSystems Institute, University of California Los Angeles, CA 90095, USA

[4]Department of Physiology, University of California Los Angeles, CA 90095, USA

[5]Interdepartmental Program in Molecular, Cellular, and Integrative Physiology, University of California, Los Angeles, California 90095, USA

[6]Department of Physics, Institute for Nanotechnology and Advanced Materials, Bar-Ilan University, Ramat-Gan, 52900, ISRAEL

[7]The Broad Institute of MIT and Harvard, Cambridge, MA 02142, USA

[8]Department of Biological Engineering, Massachusetts Institute of Technology, Cambridge, MA 02139, USA

[9]Department of Biological Chemistry, The Alexander Silberman Institute of Life Sciences, The Hebrew University of Jerusalem, Jerusalem 91904, ISRAEL

* To whom correspondence should be addressed. Tel: +1) 310-794-0093, Fax: +1) 310-267-4672, Email: sweiss@chem.ucla.edu. Correspondence may also be addressed to gelbart@chem.ucla.edu.

1. Analysis of µsALEX-FAMS data for transcription assays:

In order to select FRET-only populations and reduce possible artifacts due to dye photophysics, we implemented a dual-channel burst search (DCBS; selection of bursts which have photon emissions during their donor excitation and acceptor excitation periods)(1) for further analysis. Each burst is identified only when m(=10) consecutive photons are detected with a photon count rate that is F(=6) times higher than the background (BG) rate(2, 3). Since the BG can vary during a measurement, we computed BG rates for 30-seconds consecutive windows and applied these temporally-varying background rates to the burst search within each time window(1). We also conducted an all-photon-burst search (APBS) in order to estimate correction factors such as leakage, direct excitation, and gamma factor (γ ~0.72). These corrections were calculated according to Lee et. al.(4) and used for the burst selection following the initial DCBS selection. In the second step, only bursts that met the following criteria were kept for further analysis:

1. $n_{DD} + (1/\gamma) n_{DA} \geq 20$
2. $n_{AA} \geq 20$
3. $0.2 \leq S \leq 0.85$

Here n_{DD} or n_{DA} are the BG corrected number of photons collected from the donor or acceptor channel, respectively, during the donor excitation period, and n_{AA} is the BG corrected number of photons collected from the acceptor channel during the acceptor excitation period).

The FRET efficiency (E) and the Stoichiometry (S) for each burst were tabulated in a 2D scatter plot of E vs. S for all selected burst events. The sub-populations associated with the free ssDNA probe (high FRET efficiency) and the hybridized probe (low FRET efficiency) were identified in the 2D E-S scatter plot. 1D-FRET histograms were extracted from the 2D E-S scatter plot (as 1D projection on the E axis). For quenched-kinetics transcription assays, 1D-FRET histograms of all time points were globally fitted to a sum of two Gaussians with the shared mean FRET efficiencies and distribution widths throughout the set of data measured on the same day as constraints to the fit.

2. Validation of *in vitro* single-round quenched transcription assay:

In order to validate the *in vitro* single-round quenched transcription assay, three important controls were done: the first ensured that the probe hybridizes specifically to RNA transcripts produced by the reaction (with no non-specific binding); the second ensured that the reaction is stopped immediately when the quencher is added to the solution (fast/efficient quenching); and the last ensured that the hybridization should not be affected by crowding conditions (no hybridization bias). Transcription reactions were performed by adding NTPs to $RP_{ITC=2}$. The reactions were quenched at different time points by addition of Guanidium Chloride (GdmCl) to a final concentration of 500 mM. At this high ionic strength, RNAP-Promoter complexes are fully dissociated(5, 6). Quantification of number of transcripts per (quenched) time points was done by ALEX-FAMS measurements on hybridized probes (to transcripts)(6–8). Since the conformation of the donor (D) – acceptor (A) doubly-labeled probe changes from coiled-coil (when not hybridized) to a stretched conformation (when hybridized), the ratio between the low FRET (hybridized) sub-population to the sum of low FRET (hybridized) + high FRET (non-hybridized) sub-populations is proportional to the number of transcripts in the solution.

Only a high FRET sub-population (for the probe) was observed for the reaction mixture with no RNAP (Fig. S2A) or no NTPs (Fig. S2B), confirming that the probe binds to transcripts produced by the

transcription reaction we initiated. Fig. S3 shows no hybridized sub-population when GdmCl and NTPs are simultaneously added to the solution, suggesting full quenching of the reaction.

To rule out the possibility that addition of GdmCl does not fully quench the transcription reaction, but instead just slows it down, we measured the number of transcripts at different time points after addition of 500 mM GdmCl. As shown in Fig. S3, the number of measured transcripts measured 3 hours after NTPs and GdmCl addition (to $RP_{ITC=2}$) is the same as measured after 1 hours. We conclude that 500 mM GdmCl works as a fast and efficient quencher that completely inhibits the transcription reaction(5, 6).

Since single round quenched kinetics assay is based on hybridization reactions, it is crucial to confirm that hybridization efficiency is not affected by crowing conditions. Fig. S4 demonstrated that with our assay scheme the hybridization efficiency is consistent regardless of crowding conditions.

3. Analysis of FCS measurements for estimation of microviscosities:

The obtained correlation curves were fitted to a 3D-Gaussian Triplet model (Eq.S1) using a Python package lmfit (zenodo.org/record/11813) to extract τ_D, the resident time of the species in the focal volume (Fig S11):

$$G(\tau) = (1 - T - T \cdot e^{-\frac{\tau}{\tau^{triplet}}}) \frac{1}{N} \left(\frac{1}{1 + \frac{\tau}{\tau_D}} \right) \left(\frac{1}{1 + \frac{\tau}{K^2 \cdot \tau_D}} \right)^{1/2} \qquad \text{(Eq. S1)}$$

where N is the average number of fluorescent species in the detection volume, T is the fraction of molecules in dark state, $\tau_{triplet}$ is the life time of molecules in the dark state, and K is the structural parameter of the Gaussian detection volume profile.

Since τ_D is inversely proportional to the diffusion coefficient and directly proportional to the friction (*i.e.* viscosity) at the same temperature and the fixed detection volume, we used Eq.S2 to estimate microviscosities of complexes under crowding conditions at a given temperature T ($\eta(\mathrm{micro})_{\mathrm{Crowder,\ at\ T}}$).

$$\eta(\mathrm{micro})_{\mathrm{Crowder\ at\ T}} = \frac{\tau_{D,\mathrm{Crowder}}}{\tau_{D,\mathrm{buffer}}} \cdot \eta(\mathrm{macro})_{\mathrm{buffer\ at\ T}} \qquad \text{(Eq. S2)}$$

where $\eta(\mathrm{macro})_{\mathrm{buffer\ at\ T}}$ is the macroviscosity for the buffer at a given temperature T, $\tau_{D,\mathrm{Crowder}}$ and $\tau_{D,\mathrm{buffer}}$ are the resident times of the sample species in the presence or absence (in buffer) of crowder, respectively.

Stokes radius, R_H, of $RP_{ITC=2}$ (8.1 nm) was estimated by FCS measurements of $RP_{ITC=2}$ (cross-correlation curves of Green and Red emissions at Green laser excitation (532nm)), 20dT probe (correlation curves of Red emissions at Red (639nm) excitation, cross-correlation curves of Green and Red emissions at Green laser excitation) and Alexa 647 (correlation curves of Red emissions at Red excitation) with Eq. S3, and diffusion coefficient, D, of Alexa 647 in water ($3.25 \pm 0.1 * 10^{-10}$ m^2sec^{-1}, at 298.15 K) obtained from ref(9)

$$R_H = \frac{k_B T}{6\pi\eta D} \quad \text{for} \quad D = \frac{\omega_0^2}{4\tau_D} \qquad \text{(Eq. S3)}$$

where ω_0 is a radius of the *x-y* plane of a focal volume, k_B is the Boltzmann constant, and η is the viscosity of the medium.

We found that it is challenging to measure microviscosities of RNAP-Promoter complexes in the presence of PEG, especially at high concentrations, due to aggregation of complexes (Figs. 5, S7 and S8). It has been reported that the difference between macroviscosity and microviscosity becomes significant when the size of the crowder is similar to that of the probe molecule, and that this difference gets larger as the size of the crowder increases(10). We confirmed that microviscosities of $RP_{ITC=2}$ complexes under PEG8000 (up to 5% w/v, average M.W. ~8 kDa) and Dextran10 (average M.W. ~10 kDa) are comparable to their macroviscosities (Fig. S7A). We therefore assumed that microviscosities for crowding conditions where the crowders are smaller than PEG 8000 are the same as their macroviscosities. For larger crowders such as Ficoll 70 (average M.W. ~70 kDa) and Dextran 500 (average M.W. ~500 kDa), we used microviscosity values estimated from FCS measurements since experimental results showed clear differences (Fig. S7B).

4. Estimation of volume occupancies of the crowders:

Volume occupancies of crowding agents were calculated by the equation below using hydrodynamic radii $\boldsymbol{R_H}$ obtained from Table S1.

$$\phi_c = \frac{4\pi(R_H)^3 N_A C}{3M_W} \qquad \text{(Eq. S4)}$$

where $\boldsymbol{N_A}$ is Avogadro's number, M_W the molecular weight and **C** is the concentration (w/v) of the crowding agent.

The hydrodynamic radii of all crowders used for the calculating volume occupancies appear in Table S1.

5. Rationale for unidirectional first-order kinetics as a model for transcription after open-bubble formation:

Assuming that there is no significant pausing in elongation, the widely accepted kinetics model for transcription by *E.coli* RNAP is depicted in Figure S9(11–13). In this study, the assumption is valid due to (i) there is no known sequence for the promoter proximal pausing in the sequence of the template DNA, and (ii) the size of the elongation region is too small (< 28bp, Fig. S1) to cause a stochastically paused or arrested RNAP-DNA complex in elongation(14, 15).

Therefore, and as shown in Figure S9, promoter escape is the only rate-limiting step of the transcription reaction after open-bubble formation. In addition, it is highly unfavorable for RNAP to return back to the initiation stages once it is in the elongation stages. We therefore describe the transcription kinetics starting from an $RP_{ITC=2}$ as a unidirectional first-order process as shown in Figure 2A.

A high concentration of NTPs (at least 10^5 times higher concentration than RNAP-DNA complexes) was used so that the NTP concentration would not be limiting and hence would not affect the first-order kinetics approximation (*i.e.* Pseudo unimolecular Reaction).

The kinetic data obtained from the quenched-kinetics assays was therefore fitted to the unidirectional first-order kinetics rate equation for the extraction of kinetic parameters.

$$\left[\text{Transcript}_{\text{M}}\right]_t = \left[\text{Transcript}_{\text{M}}\right]_\infty - \left[\text{Transcript}_{\text{M}}\right]_\infty e^{-kt} \qquad \text{(Eq. S5)}$$

where $\left[\text{Transcript}_{\text{M}}\right]_t$ is the concentration of RNA transcripts produced by transcription during a given time ***t*** in the reaction medium (M = Crowder (C), Buffer (B)).

6. Estimation of the transcription rate constant from a single time point (*t*=900 sec) measurement:

Starting from $RP_{ITC=2}$, the transcription reaction can be approximated to be a first-order unidirectional reaction (Fig. 2A, Eq. S5):

$$\left[\text{Transcript}_{\text{M}}\right]_t = \left[\text{Transcript}_{\text{M}}\right]_\infty - \left[\text{Transcript}_{\text{M}}\right]_\infty e^{-kt}$$

$$\frac{\left[\text{Transcript}_{\text{M}}\right]_t}{\left[\text{Transcript}_{\text{M}}\right]_\infty} = (1 - e^{-kt}) \qquad \text{(Eq. S5)}$$

From transcription kinetics assays under crowding, we know that the same amount of RNA is synthesized regardless of the crowder's size and / or concentration (Fig. 2B):

$$\left[\text{Transcript}_{\text{B}}\right]_\infty = \left[\text{Transcript}_{\text{C}}\right]_\infty$$

Therefore,

$$\frac{\left[\text{Transcript}_{\text{C}}\right]_t}{\left[\text{Transcript}_{\text{C}}\right]_\infty} = \frac{\left[\text{Transcript}_{\text{C}}\right]_t}{\left[\text{Transcript}_{\text{B}}\right]_\infty} = \frac{\left[\text{Transcript}_{\text{B}}\right]_t}{\left[\text{Transcript}_{\text{B}}\right]_\infty} \cdot \frac{\left[\text{Transcript}_{\text{C}}\right]_t}{\left[\text{Transcript}_{\text{B}}\right]_t} = \alpha_t \text{N}_t$$

where $\alpha_t = \frac{\left[\text{Transcript}_B\right]_t}{\left[\text{Transcript}_B\right]_\infty}$ and $\text{N}_t = \frac{\left[\text{Transcript}_C\right]_t}{\left[\text{Transcript}_B\right]_t}$

Eq. S5 could thus be re-written as:

$$\frac{\left[\text{Transcript}_{\text{M}}\right]_t}{\left[\text{Transcript}_{\text{M}}\right]_\infty} = \alpha_t \text{N}_t = (1 - e^{-kt})$$

$$e^{-kt} = 1 - \alpha_t \text{N}_t$$

$$-kt = \ln(1 - \alpha_t \text{N}_t)$$

Since $k \propto 1/\eta$ according to Kramers theory,

$$-kt = -k_0 \cdot \frac{1}{\eta_M} \cdot t = \ln(1-\alpha_t \mathrm{N}_t)$$

where η_M is the reaction medium's viscosity (i.e. buffer or crowded condition) and k_0 is a viscosity-adjusted rate constant.

Therefore, k_0 is given by:

$$k_0 = -\frac{\eta_M}{t} \ln(1-\alpha_t \mathrm{N}_t)$$

Single time-point measurements were done at 900 secs after addition of NTPs. Therefore, we plug-in t = 900 in the above equation:

$$k_0 = -\frac{\eta_M}{900} \ln(1-aR), \text{ for } a = \alpha_{900} = \frac{[\text{Transcript}_B]_{900}}{[\text{Transcript}_B]_{\infty}}, \; R = \mathrm{N}_{900} = \frac{[\text{Transcript}_C]_{900}}{[\text{Transcript}_B]_{900}} \quad \text{(Eq.S6)}$$

where η_M is the viscosity of the reaction medium (M), a is the ratio between transcription efficiency in buffer at t=900 sec and transcription efficiency in buffer after reaching a steady-state (t=∞). a is obtained from the fitted kinetic curve (red curve in Fig. 2B). R is the ratio of transcription efficiency in the crowded medium at t=900 sec to that in buffer at the same time point, obtained from Figs. 3A and 3B.

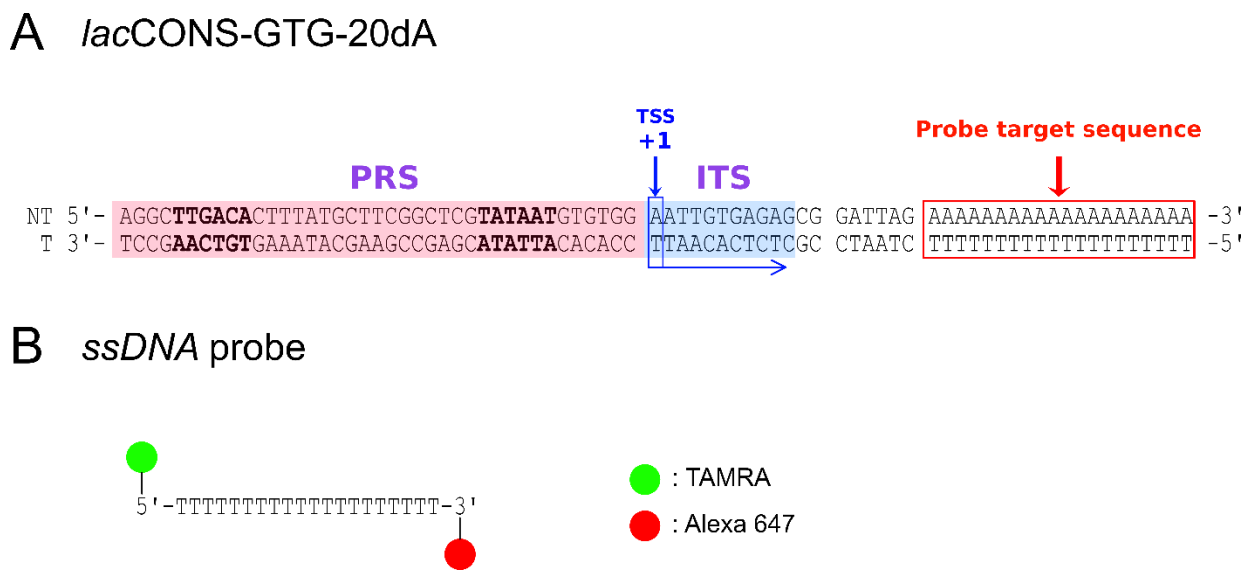

Figure S1. The sequences of *lac*CONS-GTG-20dA template and ssDNA probe used in this study. (A) Sequence of the non-template (top, NT) and template (bottom, T) strands of *lac*CONS-GTG-20dA template. The promoter recognition sequence (PRS), the Initially Transcribed Sequence (ITS), and the targeting regions are highlighted in pink, blue, and in red box respectively. The Transcription start site (TSS) and the initiating nucleotide position (+1) are marked by the blue arrow. Once RNAP finishes transcribing the template strand into RNA, the RNA will contain 20 consecutive A's (20dA). (B) This 20dA part of transcribed RNA is detected by the doubly labeled ssDNA probe.

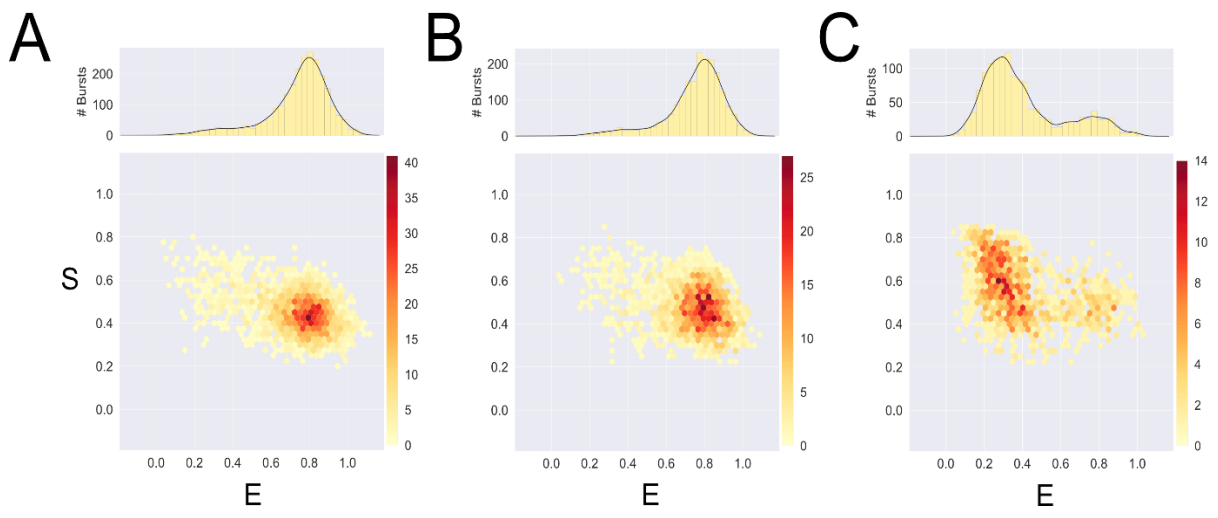

Figure S2. Controls for *in vitro* single-round quenched transcription assay. The high FRET sub-population shifts toward a low FRET sub-population upon probe hybridization with RNA transcripts. (A) no RNAP negative control; A solution containing ssDNA probe, promoter DNA, and NTPs was incubated for 15 min at 37˚C, then quenched by 500 mM GdmCl. (B) no NTP negative control; A solution containing ssDNA probe, and RNAP-Promoter open complexes ($RP_{ITC=2}$) was incubated for 15 min at 37˚C, then quenched by 500 mM GdmCl. (C) Positive control; A solution containing ssDNA probe, $RP_{ITC=2}$, and 100μM NTPs was incubated for 15 min at 37˚C, then quenched by 500 mM GdmCl.

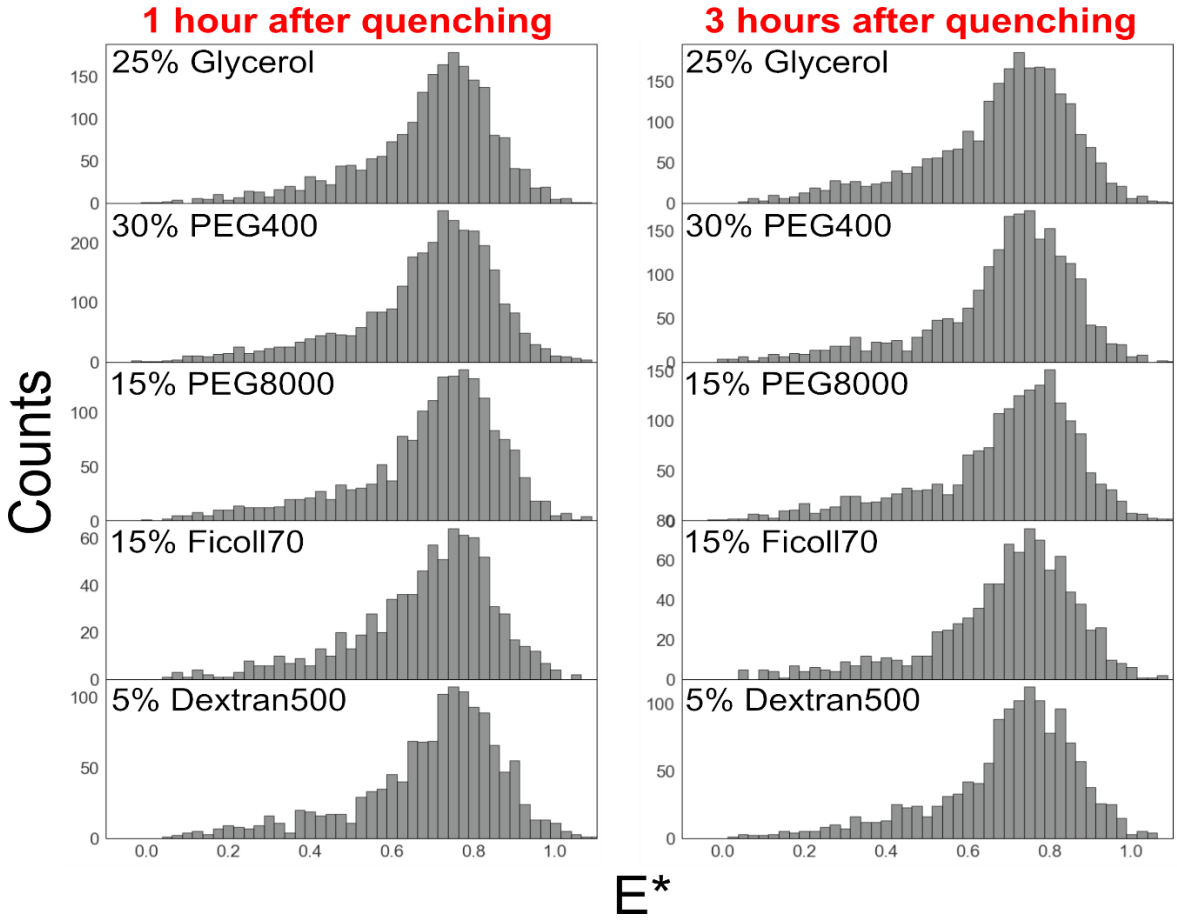

Figure S3. 500 mM GdmCl acts as an efficient quencher for the *in vitro* single-round quenched transcription assay (for various crowding environments). FRET histograms for transcription reactions that were immediately quenched by 500 mM GdmCl followed by addition of NTPs (0 min incubation). Transcription reactions quenched at 0 min in various crowding conditions were measured by ALEX-FAMS 1 hour after quenching (left column), or 3 hours after quenching (right column).

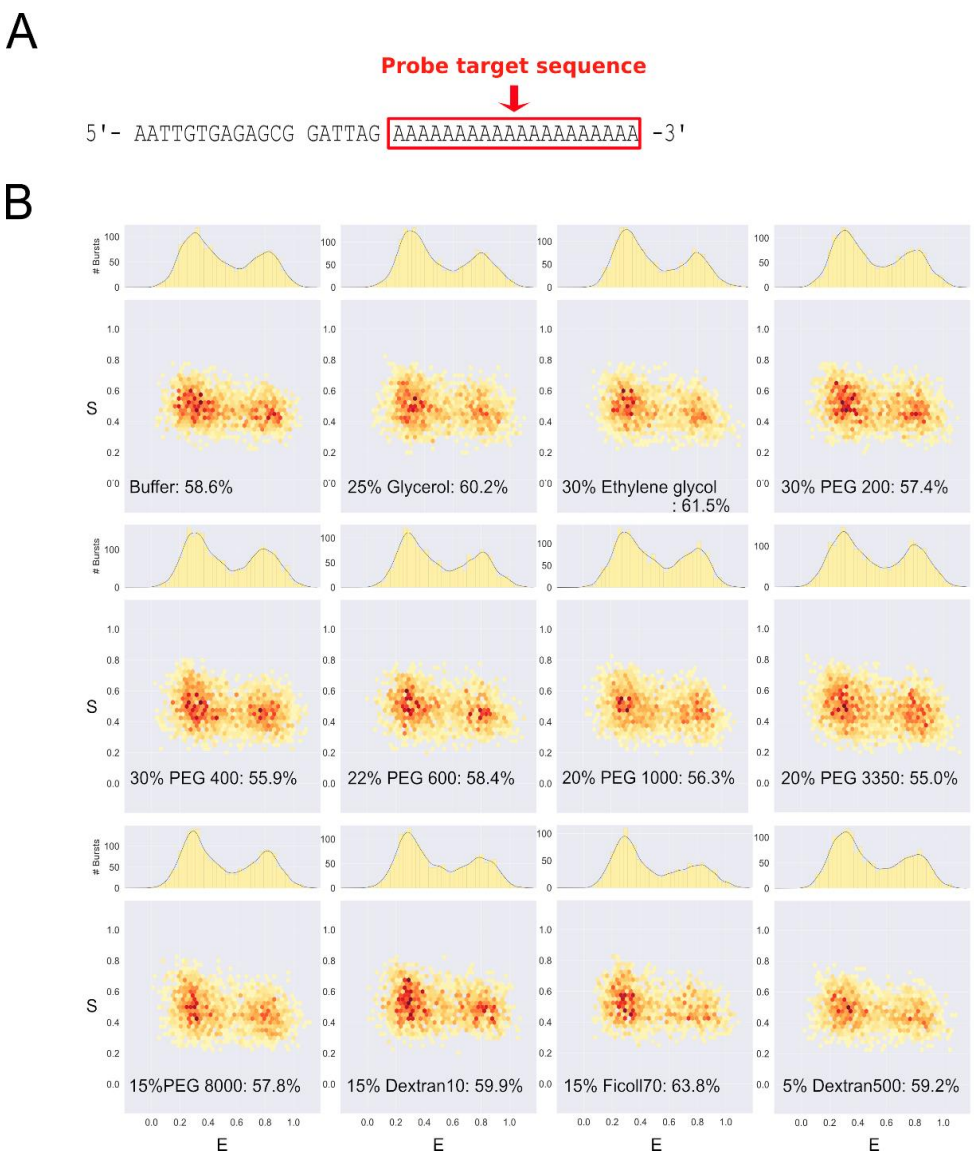

Figure S4. Hybridization of ssDNA transcript mimic and fluorescence probe under various crowding conditions. (A) The sequence of ssDNA as a transcript mimic used in the hybridization assays. The sequence stems from the transcribing region of *lac*CONS-GTG-20dA template. (B) FRET histograms for hybridization reactions of ssDNA transcript mimic and probe under various crowding conditions. The reactions were initiated by adding 1.5X volumes of quencher/probe solution containing 1.25 M Guanidium Chloride (GdmCl) and 250 pM ssDNA probe to 1 volume of solution containing ssDNA mimic and crowders. The assays showed no noticeable difference in hybridization efficiency throughout all crowding conditions.

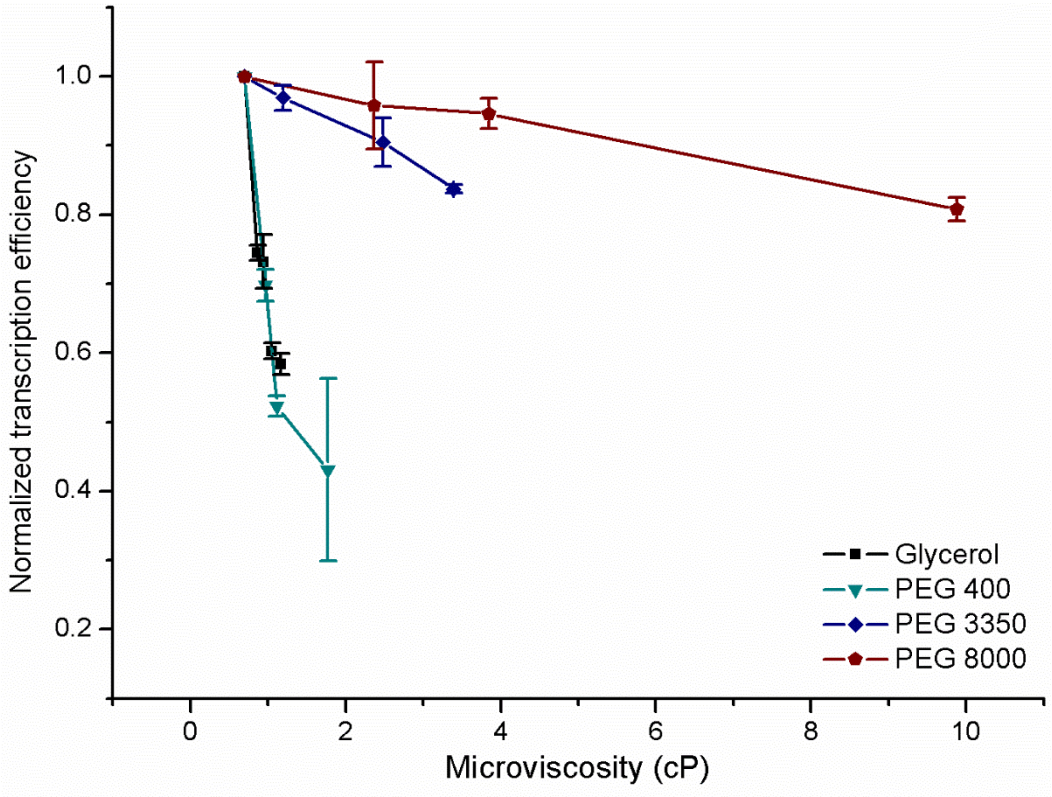

Figure S5. Normalized transcription efficiencies (at a single time point, $t_{incubation}$= 900s) for different crowders, as a function of viscosity. RNA- binding dye assay. Transcription efficiency values are normalized to the reaction without crowders (buffer only). Error bars represent standard deviations of triplicates from their mean values.

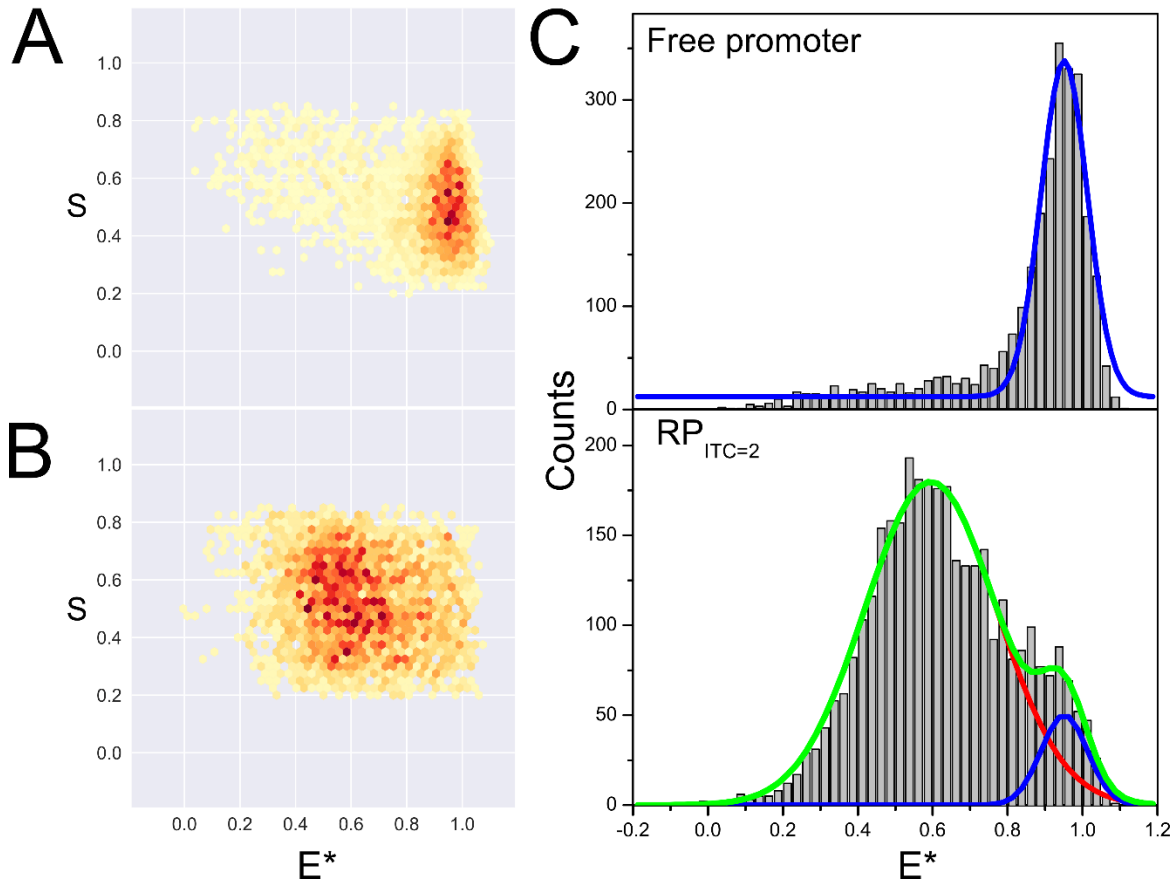

Figure S6. RNAP-promote open complex ($RP_{ITC=2}$) is the major species in the reaction mixture used for FCS measurements. Samples prepared for FCS analysis were first examined by μsALEX-FAMS. E-S histograms for (A) a solution containing dual-labeled *lac*CONS-GTG-20dA promoter DNA only (No RNAP was added); (B) a solution containing dual-labeled *lac*CONS-GTG-20dA promoter DNA with added RNAP. The major species is $RP_{ITC=2}$ (with E~0.6) (the reaction mixture contained RNAP, Promoter DNA, and ApA(6, 16)); (C) 1D FRET histograms for (A) (promoter DNA only, top), and for (B) ($RP_{ITC=2}$ reaction mixture, bottom). $RP_{ITC=2}$ reaction mixture was estimated to contain ≥ 90% of the major species by fitting with the sum (green) of two Gaussian curves (blue for free promoter DNA and red for $RP_{ITC=2}$)

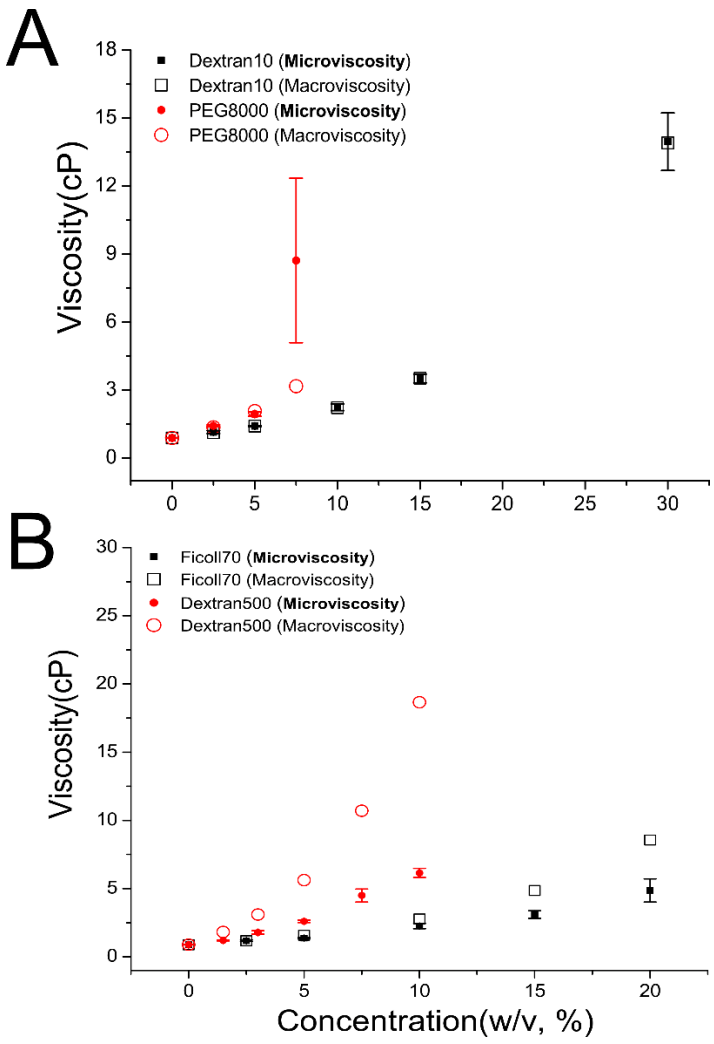

Figure S7. Microviscosities for RNAP-Promoter complexes under various crowding conditions measured by FCS. (A) Microviscosities estimated for various concentrations of Dextran 10 and PEG8000. At 7.5% PEG 8000, $RP_{ITC=2}$ mixture started to exhibit aggregation (see main text), leading to large errors in microviscosity estimation; (B) Microviscosities estimated for large crowders (Dextran 500, red and Ficoll 70, black). Estimated microviscosities (filled circle and square) are noticeably different from their macroviscosities (open circle and square), especially at high concentrations. Error bars represented standard deviations of triplicate measurements.

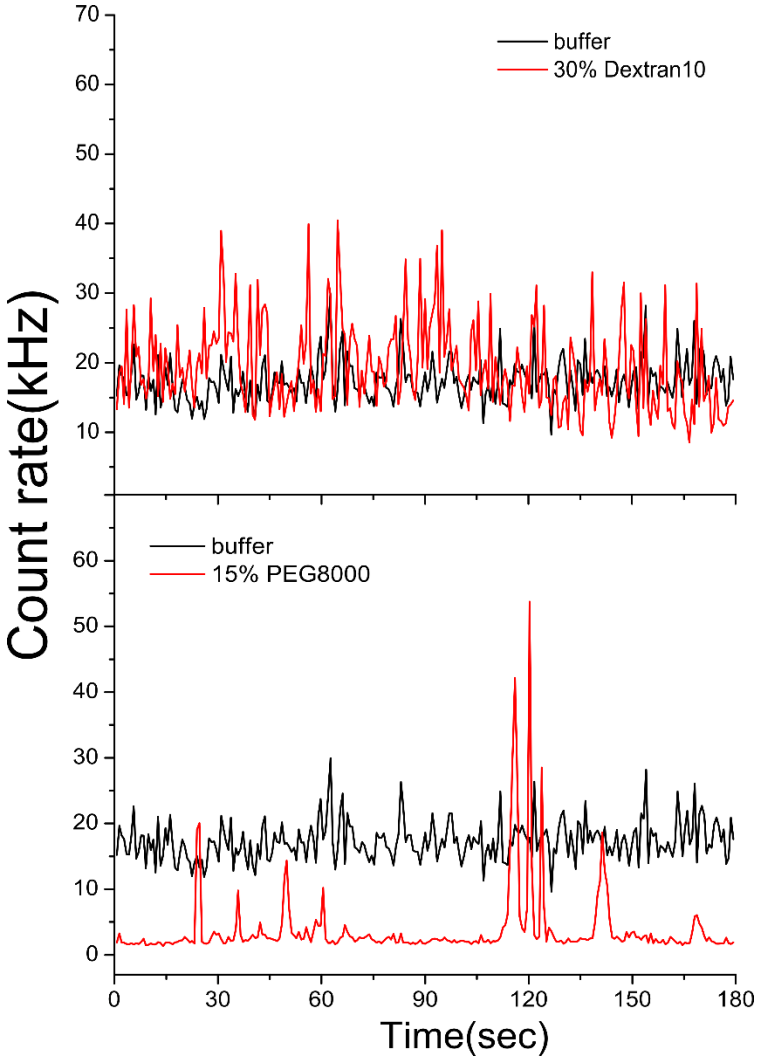

Figure S8. Comparisons of photon emission rate trajectories for $RP_{ITC=2}$ in 30% Dextran10 (top) and 15% PEG8000 (bottom) to the same in buffer. Although the macroviscosities for 30% Dextan10 and 15% PEG8000 are similar, the photon emission rate trajectories (of $RP_{ITC=2}$) are significantly different: For 15% PEG8000 (bottom), a lower background (base) photon emission rate with frequent large spikes is observed (as compared to the same in buffer). For 30% Dextran10 (top), the photon emission rate is similar (but noisier) to the same in buffer.

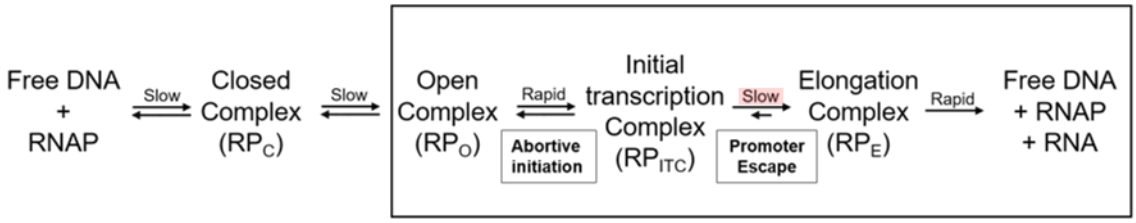

Figure S9. The widely accepted kinetic model for transcription *E.coli*. RNAP. According to the model, the promoter escape is the only slow (*i.e.* rate limiting, highlighted in red) step after open complex formation(11–13).

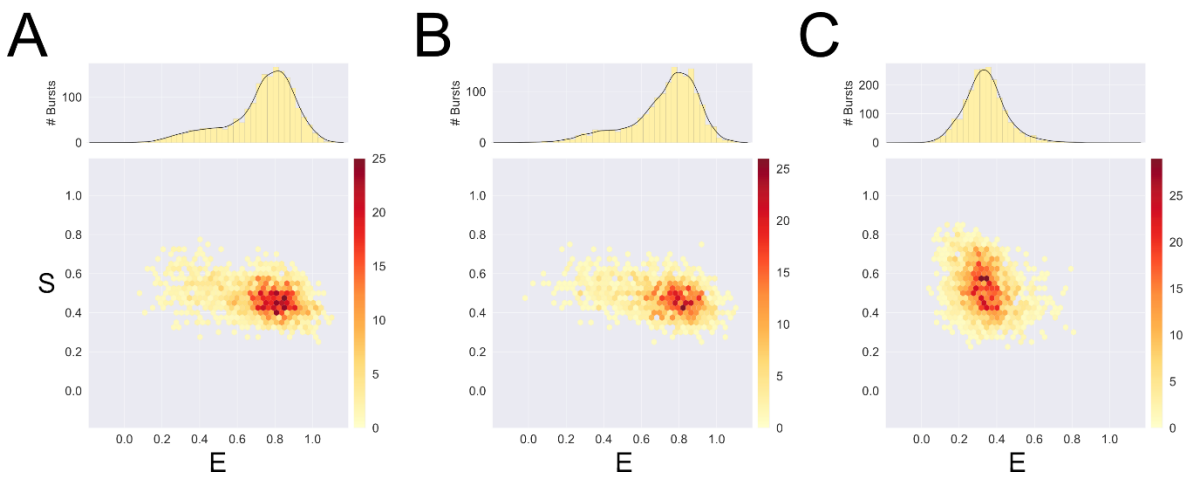

Figure S10. Single point (t=900s) transcription assays starting from RNAP-DNA association. (A) 15min incubation of free 25nM RNAP holoenzyme and free 1nM *lac*CONS-GTG-20dA template DNA without NTPs in transcription buffer (no NTP control). (B) 15min incubation of free 1nM RNAP holoenzyme and free 1nM *lac*CONS-GTG-20dA template DNA with 100μM NTPs in transcription buffer. (C) 15min incubation of free 25nM RNAP holoenzyme and free 1nM *lac*CONS-GTG-20dA template DNA with 100μM NTPs in transcription buffer. The assays demonstrated that no noticeable transcription (starting from DNA-RNAP binding & transcription open bubble formation) takes place during 15 min incubation time at 1nM RNAP and 1nM DNA while 25nM RNAP and 1nM DNA produce notable amount of RNA transcripts.

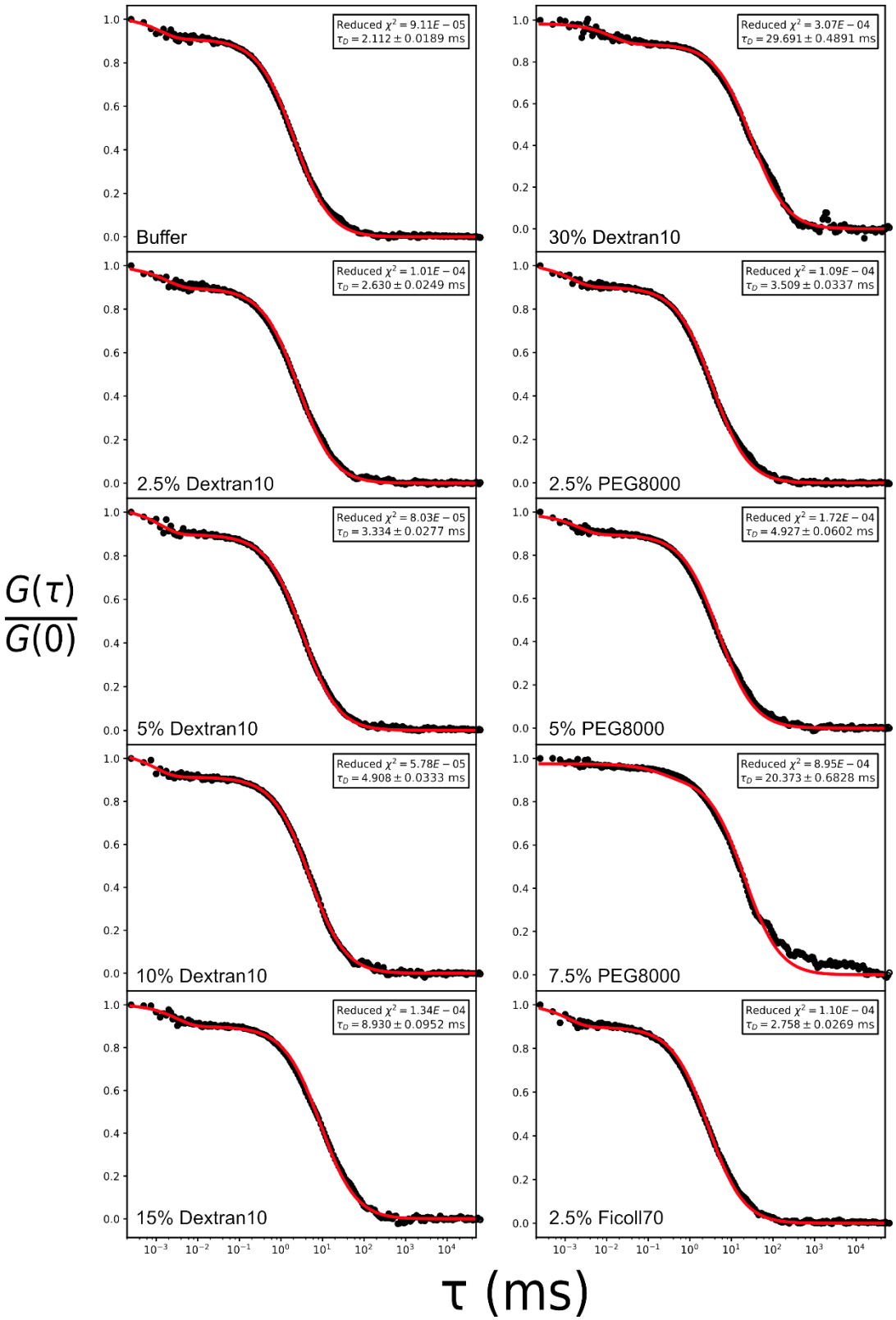
Reduced $\chi^2 = 9.11E-05$
$\tau_D = 2.112 \pm 0.0189$ ms
Buffer
Reduced $\chi^2 = 3.07E-04$
$\tau_D = 29.691 \pm 0.4891$ ms
30% Dextran10
Reduced $\chi^2 = 1.01E-04$
$\tau_D = 2.630 \pm 0.0249$ ms
2.5% Dextran10
Reduced $\chi^2 = 1.09E-04$
$\tau_D = 3.509 \pm 0.0337$ ms
2.5% PEG8000
Reduced $\chi^2 = 8.03E-05$
$\tau_D = 3.334 \pm 0.0277$ ms
5% Dextran10
Reduced $\chi^2 = 1.72E-04$
$\tau_D = 4.927 \pm 0.0602$ ms
5% PEG8000
Reduced $\chi^2 = 5.78E-05$
$\tau_D = 4.908 \pm 0.0333$ ms
10% Dextran10
Reduced $\chi^2 = 8.95E-04$
$\tau_D = 20.373 \pm 0.6828$ ms
7.5% PEG8000
Reduced $\chi^2 = 1.34E-04$
$\tau_D = 8.930 \pm 0.0952$ ms
15% Dextran10
Reduced $\chi^2 = 1.10E-04$
$\tau_D = 2.758 \pm 0.0269$ ms
2.5% Ficoll70
$\frac{G(\tau)}{G(0)}$
τ (ms)

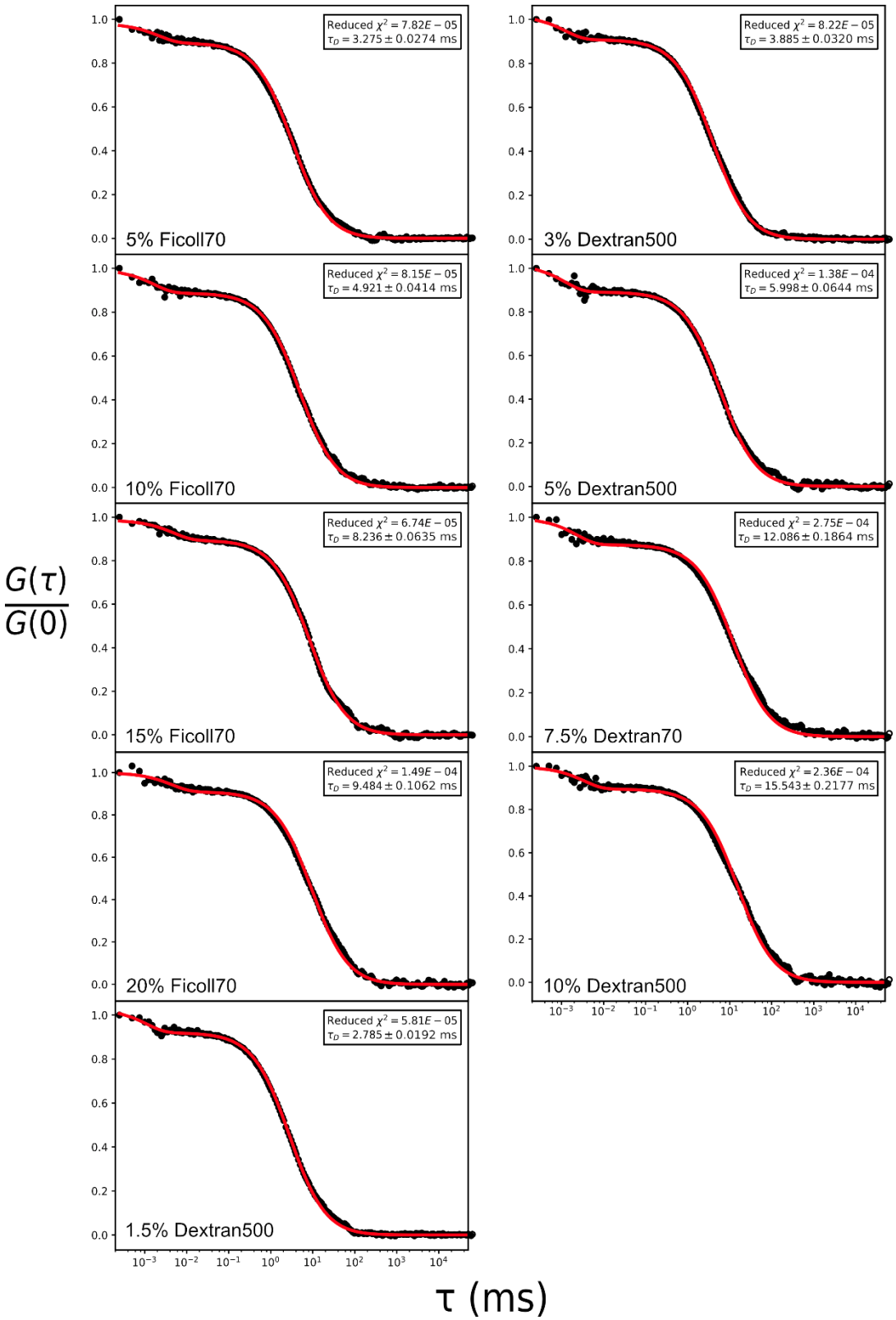

Figure S11. Fluorescence correlation data for $RP_{ITC=2}$ under various crowding conditions (black dots) and their fitting curves (red line) with the model.

Table S1. Hydrodynamic radii of crowding agents used in this study

Crowding agent	Average Molecular Weight (g/mol)	Hydrodynamic radius (Å)
Ethylene Glycol	62.07	2.2
Glycerol	92.09	3.1
PEG 200	200	4.0
Sucrose	342.30	4.9
PEG 400	400	5.6
PEG 600	600	6.9
PEG 1000	1000	8.9
PEG 3350	3350	16.1
Dextran 5	5000	16.6
Dextran 10	10000	24.0
PEG 8000	8000	26.6
Ficoll 70	74000	55.0
Dextran 500	500000	165.0

Hydrodynamic radii of all crowders were obtained from references(17–21).

References

1. Nir,E., Michalet,X., Hamadani,K.M., Laurence,T.A., Neuhauser,D., Kovchegov,Y. and Weiss,S. (2006) Shot-noise limited single-molecule FRET histograms: comparison between theory and experiments. *J. Phys. Chem. B*, **110**, 22103–24.

2. Eggeling,C., Berger,S., Brand,L., Fries,J.R., Schaffer,J., Volkmer,A. and Seidel,C.A. (2001) Data registration and selective single-molecule analysis using multi-parameter fluorescence detection. *J. Biotechnol.*, **86**, 163–80.

3. Michalet,X., Colyer,R.A., Scalia,G., Ingargiola,A., Lin,R., Millaud,J.E., Weiss,S., Siegmund,O.H.W., Tremsin,A.S., Vallerga,J. V, *et al.* (2012) Development of new photon-counting detectors for single-molecule fluorescence microscopy. *Philos. Trans. R. Soc. B Biol. Sci.*, **368**, 20120035–20120035.

4. Lee,N.K., Kapanidis,A.N., Wang,Y., Michalet,X., Mukhopadhyay,J., Ebright,R.H. and Weiss,S. (2005) Accurate FRET measurements within single diffusing biomolecules using alternating-laser excitation. *Biophys. J.*, **88**, 2939–2953.

5. Das,M. and Dasgupta,D. (1998) Enhancement of transcriptional activity of T7 RNA polymerase by guanidine hydrochloride. *FEBS Lett.*, **427**, 337–40.

6. Lerner,E., Chung,S., Allen,B.L., Wang,S., Lee,J., Lu,S.W., Grimaud,L.W., Ingargiola,A., Michalet,X., Alhadid,Y., *et al.* (2016) Backtracked and paused transcription initiation intermediate of Escherichia coli RNA polymerase. *Proc. Natl. Acad. Sci. U. S. A.*, **113**, E6562–E6571.

7. Kapanidis,A.N., Lee,N.K., Laurence,T.A., Doose,S., Margeat,E. and Weiss,S. (2004) Fluorescence-aided molecule sorting: analysis of structure and interactions by alternating-laser excitation of single molecules. *Proc. Natl. Acad. Sci. U. S. A.*, **101**, 8936–41.

8. Kim,S., Streets,A.M., Lin,R.R., Quake,S.R., Weiss,S. and Majumdar,D.S. (2011) High-throughput single-molecule optofluidic analysis. *Nat. Methods*, **8**, 242–5.

9. Loman,A. (2010) Molecular Sizing using Fluorescence Correlation Spectroscopy.

10. Kalwarczyk,T., Ziębacz,N., Bielejewska,A., Zaboklicka,E., Koynov,K., Szymański,J., Wilk,A., Patkowski,A., Gapiński,J., Butt,H.J., *et al.* (2011) Comparative analysis of viscosity of complex liquids and cytoplasm of mammalian cells at the nanoscale. *Nano Lett.*, **11**, 2157–2163.

11. Bai,L., Shundrovsky,A. and Wang,M.D. (2009) Kinetic Modeling of Transcription Elongation. In *RNA Polymerases as Molecular Motors*.

12. Geszvain,K.. and Landick,R. (2004) The structure of bacterial RNA polymerase. In *The bacterial chromosome*.pp. 283–296.

13. Dangkulwanich,M., Ishibashi,T., Bintu,L., Bustamante,C. and Choy,J.L. (2014) Molecular mechanisms of transcription through single-molecule experiments. *Chem. Rev.*, **114**, 3203–3223.

14. Shaevitz,J.W., Abbondanzieri,E. a, Landick,R. and Block,S.M. (2003) Backtracking by single RNA polymerase molecules observed at near-base-pair resolution. *Nature*, **426**, 684–687.

15. Neuman,K.C., Abbondanzieri,E.A., Landick,R., Gelles,J. and Block,S.M. (2003) Ubiquitous Transcriptional Pausing Is Independent of RNA Polymerase Backtracking. *Cell*, **115**, 437–447.

16. Lerner,E., Ingargiola,A., Lee,J.J., Borukhov,S., Michalet,X. and Weiss,S. (2017) Different types of pausing modes during transcription initiation. *Transcription*, **8**, 242–253.

17. Kuga,S. (1981) Pore size distribution analysis of gel substances by size exclusion chromatography. *J. Chromatogr. A*, **206**, 449–461.

18. Devanand,K. and Selser,J.C. (1991) Asymptotic Behavior and Long-Range Interactions in Aqueous Solutions of Poly(ethylene oxide). *Macromolecules*, **24**, 5943–5947.

19. Schultz,S.G. and Solomon,A.K. (1961) Determination of the effective hydrodynamic radii of small molecules by viscometry. *J. Gen. Physiol.*, **44**, 1189–99.

20. van den Berg,B., Wain,R., Dobson,C.M. and Ellis,R.J. (2000) Macromolecular crowding perturbs protein refolding kinetics: implications for folding inside the cell. *EMBO J.*, **19**, 3870–3875.

21. Aimar,P., Meireles,M. and Sanchez,V. (1990) A contribution to the translation of retention curves into pore size distributions for sieving membranes. *J. Memb. Sci.*, **54**, 321–338.